ORIGINAL ARTICLE

A C G publications

Org. Commun. 18:4 (2025) 307-320

organic communications

Synthesis and molecular docking studies of dispiropyrrolidine oxindole derivatives as a therapeutics agent against methicillin-resistant *Staphylococcus aureus* (MRSA)

Mohd Khairul Nizam Mazlan [1,2,3,4], Mohamad Nurul Azmi [4*], Saiful Azmi Johari [5], Nor Syaidatul Akmal Mohd Yousof [6], Mohammad Tasyriq Che Omar [7], Habibah A. Wahab [8] and Mohd Fazli Mohammat [1,2*]

[1]*Organic Synthesis Research Laboratory, Institute of Science (I.O.S), Universiti Teknologi MARA, 42300 Bandar Puncak Alam, Selangor, Malaysia*

[2]*Faculty of Applied Sciences, Universiti Teknologi MARA, 40450 Shah Alam, Selangor, Malaysia*

[3]*Collaborative Laboratory for Herbal Standardization (CHEST), School of Pharmaceutical Sciences, Universiti Sains Malaysia, 11900 Bukit Jambul, Penang, Malaysia*

[4]*Natural Products and Synthesis Organic Research Laboratory (NPSO), School of Chemical Sciences, Universiti Sains Malaysia, 11800 Minden, Penang, Malaysia*

[5]*Antimicrobial Laboratory, Anti-Infective Branch, Bioactivity Programme, Natural Products Division, Forest Research Institute Malaysia (FRIM), 52109 Kepong, Selangor, Malaysia*

[6]*Herbal Medicine Research Centre, Institute for Medical Research (IMR), National Institutes of Health (NIH), Setia Alam, 40170 Shah Alam, Selangor, Malaysia*

[7]*Biological Section, School of Distance Education, Universiti Sains Malaysia, 11800 Minden, Penang, Malaysia*

[8]*Pharmaceutical Design and Simulation Laboratory, School of Pharmaceutical Sciences, Universiti Sains Malaysia, 11800 Minden, Penang, Malaysia*

(Received November 16, 2025; Revised December 12, 2025; Accepted December 20, 2025)

Abstract: A series of new dispiropyrrolidine oxindole derivatives (**8-10**) were successfully synthesised with yield of 57 to 95% via one-pot 1,3-dipolar cycloaddition reaction of azomethine ylides and characterised by various spectroscopic techniques such as NMR, FT-IR, and HRMS. The compounds were evaluated for their activity against methicillin-resistance *Staphylococcus aureus* (MRSA). Among the compounds, compound **9f** and **9g** exhibit moderate activity against MRSA with minimum inhibitory concentration (MIC) and minimum bactericidal concentration (MBC) of 250 µg/mL and 325 µg/mL, respectively. The binding energies and interactions of both compounds with *S. aureus* adhesion proteins such as sdrE, CIfA and FnBPA were further studied through molecular docking studies. Compound **9f** (-8.5 ± 0.00 kcal/mol) showed a strong binding affinity than compound **9g** (-7.5 ± 0.20 kcal/mol) particularly towards FnBPA adhesion protein. The molecular docking results revealed that the interactions between the compounds **9f** and **9g** with target proteins correlate with the observed MRSA inhibitory activity, highlighting their potential as promising lead candidates for anti-MRSA drug development.

Keywords: Dispiropyrrolidine oxindole; anti-bacterial activity; methicillin-resistant *Staphylococcus aureus*; molecular docking; i*n silico* study.

* Corresponding author: E-Mail: mohdfazli@uitm.edu.my, mnazmi@usm.my, Phone: +60355211354

The article was published by ACG Publications
http://www.acgpubs.org/journal/organic-communications © July-December 2025 EISSN:1307-6175
DOI: http://doi.org/10.25135/acg.oc.204.2511.3729
Availeble online: Decemebr 26, 2025

1. Introduction

Methicillin-resistant *Staphylococcus aureus* (MRSA) represents a critical threat to global public health, characterised by high mortality and morbidity rates[1]. In 2024, MRSA has been classified as a global issue with a high burden and drug-resistant bacteria by the World Health Organization (WHO)[2]. According to the National Antibiotic Resistance Surveillance (NARS) Report 2024 by the Ministry of Health Malaysia, MRSA threat rates are increased from 7% in 2021 to 9.4% in 2024 which most cases are from medical, surgical and intensive care wards[3]. This threat arises from MRSA resistance to multiple classes of antibiotics. Since the early 1960s, MRSA has progressively evolved and adapted to evade beta-lactam[4] and other classes of antibiotics, including macrolides[5], aminoglycosides[6], fluoroquinolones[7], and glycopeptides[8]. MRSA host interaction that caused infection and adaptation to multiple classes of antibiotics contributes to the high mortality rate around the world, making it a significant global health challenge.

The current treatment of MRSA as recommended by the Infectious Diseases Society of America (IDSA) recommends vancomycin or daptomycin as first line therapeutic agent[9]. However, the limitation of these drugs are adverse side effects such as acute kidney injury[10] and rhabdomyolysis with increasing creatine phosphokinase at a higher dose[11]. In 2010, ceftaroline, a β-lactam antibiotic, was approved by the United States Federal Drug Administration (USFDA) to manage acute bacterial skin and community-acquired bacterial pneumonia due to MRSA. However, the adverse side effect arises when ceftaroline is prescribed for more than seven days or at higher dosage[12]. Thus, MRSA infection is continuously a growing burden worldwide and has significantly reduced available therapeutic options. Hence, there is an urgent need for developing multi-drug strategies for the treatment of MRSA.

Recently, we have highlighted the potential of acetoxychavicol acetate and its derivatives in inhibiting MRSA with *in silico* molecular modelling study on three adhesion protein of *Staphylococcus aureus*[13]. Three molecular adhesion protein are serine-aspartate repeat-containing protein E (sdrE), clumping factor A (ClfA) and fibronectin-binding protein A (FnBPA) belong to microbial surface component recognising adhesive matrix molecules (MSCRAMMs) which have unique roles in the interaction of *Staphylococcus aureus* to bind with host cells[14, 15]. Each protein contains ligand-binding domain via dynamic mechanisms such as “dock, lock, latch” models[16].

sdrE adhesion protein bind to Complement factor H ligand to help in immune evasion[15]. While for ClfA, it binds to fibrinogen ligand to initiate adhesion and biofilm formation for the infection[17]. FnBPA binds primarily to fibrinogen but can also interact with other ligands such as fibronectin and elastin, thereby enhancing the adhesion to host cells. All these three adhesion proteins are involved in forming biofilms which are important to the pathogenesis, immune evasion and virulence factor of *Staphylococcus aureus* to the host tissues[13, 18-20].

In the pursuit of developing synthetic drugs for the inhibition of *Staphylococcus aureus*, spirocyclic compounds, a molecule with at least two rings connected by a single carbon atom. This spirocyclic compound can be found in many derivatives obtained from various natural resources[21]. With their unique non-planar three-dimensional scaffold, it has been suggested that spirocyclic compound are more likely to be successfully developed as a drug than flat ring compounds[22]. Spiropyrrolidine compound are one of spirocyclic compound that have shown wide potential on biological properties on various studies. They have been well studied for various biological activities such as anti-cancer[23], anti-cholinesterase[24], anti-mycobacteria[25], anti-inflammatory[26] and anti-malarial activities[27]. Recently, spiropyrrolidine oxindole compounds have been found to be active against MRSA[28]. The enhanced biological activities of spiropyrrolidine oxindole compound might be due to their three-dimensional scaffold molecular structure which offer a better binding interaction with the active site of the targeted protein[29]. Previously, we have synthesised dispiropyrrolidine oxindole derivatives via a one-pot 1,3-dipolar cycloaddition of azomethine ylides, generated from sarcosine and isatin derivatives[24]. Hence, similar methodology and reaction mechanism from the previous study have been used and discussed as part of this work. However, in this extended study, we incorporating electron donating and withdrawing group to the dispiropyrrolidine oxindole derivatives, MRSA inhibitory biological activity and molecular docking study that has not been reported in our previous study.

2. Experimental

2.1. Chemical Material and Apparatus

Chemicals and reagents used for chemical synthesis such as 4-piperidone, (2-bromoethyl) benzene, benzaldehyde, 4-methylbenzaldehyde, 4-methoxybenzaldehyde, 2-methoxybenzaldehyde, 2,4-methoxybenzaldehyde, 4-chlorobenzaldehyde, 4-bromobenzaldehyde, 4-fluorobenzaldehyde, isatin, 5-bromoisatin, 5-fluoroisatin, sodium carbonate, and sodium hydroxide were analytical grade, purchased from Sigma-Aldrich (USA), Acros Organics (USA) and Fisher Scientific (USA). The analytical reagent grade (AR grade) solvent for reaction and purification purposes such as *n*-hexane, ethyl acetate, acetonitrile, ethanol, methanol was purchased from QReC (Malaysia) and used without further purification process. Purity of the synthesised compound and reaction progress were monitored using a thin layer chromatography (TLC) sheet precoated with silica gel 60 F_{254} (0.040-0.063 mm) purchased from Merck (Germany). The melting points were recorded using the Stuart^{tm} SMP30 melting point (Cole Palmer, USA). The Fourier-Transform Infrared (FT-IR) spectra were analysed using a Shimadzu FTIR equipped with ATR. Nuclear magnetic resonance (NMR) spectra were obtained using a 500 MHz Bruker Advance NMR (500 MHz for ^{1}H-NMR, 125 MHz for ^{13}C-NMR) spectrometer system, and the data were analysed using MNova Software Version 14.2.1 (Mestrelab Research, Santiago de Compostela, Spain). The chemical shifts were internally calibrated using DMSO-d_6 peak (^{1}H: 2.50 ppm, ^{13}C:39.5 ppm), or $CDCl_3$ peak (1H: 7.26 ppm, 13C:77.0 ppm) for both ^{1}H and ^{13}C-NMR. The mass spectra have been recorded with LC-MS Thermo UPLC Binary System (ThermoFisher Scientific, Waltham, MA, USA) equipped with QExactive™ Orbitrap Mass Spectrometer (Thermo Fisher Scientific, Waltham, MA, USA),

2.2. Chemistry

2.2.1. Synthesis of 1-phenethylpiperidine-4-one[30]

The synthesis of 1-phenethylpiperidine-4-one (**3**) was synthesised with the reaction between 4-piperidone monohydrate hydrochloride (**1**) (10 mmol, 1 equiv.), sodium carbonate (24 mmol, 2.4 equiv.) and 2-bromoethyl benzene (**2**) (12 mmol, 1.2 equiv.) in 80 mL acetonitrile. The suspension was stirred and refluxed at 65°C. After 12h, the reaction mixture was cooled to ambient temperature and extracted with dichloromethane. The organic layer was washed with water and dried over anhydrous sodium sulphate and concentrated using rotary evaporator. The resulting yellow oil was subjected to silica column chromatography (hexane/ethyl acetate 50%) to give the desired compound **3**. The details of the reactions and the spectroscopic data can be found in the Supporting Information (Figure S1-S5).

2.2.2. General Synthesis of (3E,5E)-3,5-diarylidene-1-phenethylpiperidine-4-one derivatives[31]

A mixture of 1-phenethylpiperidine-4-one (**3)** (1 mmol, 1 equiv.), appropriate aldehyde **4** (2 mmol, 2 equiv.) was dissolved in ethanol (20 mL), 10 mL of 30% sodium hydroxide solution was added dropwise over 15 minutes period and stirred with a magnetic stirrer for 2-6 hours at room temperature. After completion of the reaction as detected by TLC, the mixture was poured into crushed ice. The precipitated solid was filtered and washed with cold ethanol to obtain the final products **5a-5h**. The details of the reactions and the spectroscopic data can be found in the Supporting Information (Figure S6-S45).

2.2.3. General Procedure for Synthesis of dispiropyrrolidine oxindole Derivatives[24]

The synthesis of dispiropyrrolidine oxindole derivatives (**8a-10h**) is shown in Scheme 1. (3*E*,5*E*)-3,5-diarylidene-1-phenethylpiperidine-4-one (**5a-h**) was refluxed with appropriate isatin derivatives (**7a-c**) and sarcosine (**6**) in methanol (20 mL) for 4-7 hours. Upon completion, the reaction mixture was cooled to room temperature and poured into water (20 mL). The resulting precipitate was collected by filtration and washed with cold methanol to yield the desired compound **8a-10h**. The details of the reactions and the spectroscopic data can be found in the Supporting Information (Figure S46-S165).

2.3. Biological Assay

2.3.1. Bacterial Isolates and Growth Conditions[32]

The MRSA ATCC 25923 and ATCC 33591 was utilised and maintained in the Antimicrobial Laboratory, Forest Research Institute of Malaysia (FRIM), on Protect Bacterial Preservers (Technical Service Consultants Limited, Heywood, Lanshire, England) at -20°C. Prior to use, isolates were subculture overnight at 37°C in Mueller-Hinton broth (MHB) and adjusted to obtain turbidity comparable to McFarland standards accordingly using a cell density meter (Biochrom WPA CO8000, Cambridge, UK) at 600 nm.

2.3.2. Minimum Inhibitory Concentration (MIC) and Minimum Bactericidal Concentration (MBC) Assay

MIC and MBC assays were used to evaluate antimicrobial efficiency using agar-well diffusion method adheres to Clinical and Laboratory Standards Institute (CLSI) guidelines[32]. Serial dilution of the compound was prepared in dimethyl sulfoxide (DMSO) and tested with a microbial suspension at 108 CFU/mL at 37°C for 24 hours. The MIC value was defined as the lowest concentration of the compounds showing no visible microbial growth and MBC value was defined as the lowest concentration of the compounds to kill 99.9 % of the bacteria.

2.4. Molecular Docking Studies

In our previous work[13], we have reported molecular docking study of acetoxychavicol acetate (ACA) compounds and its analogues to *S. aureus* adhesion protein such as sdrE, CIfA and FnBPA. Hence, similar docking method and protocol have been applied for this study. The docking process began by downloading the Protein Data Bank (PDB) files (PDB ID: 5WTA, 2VR3, 4B5Z) from Protein Data Bank (http://www.rcsb.org/pdb). The DockPrep tools in UCSF Chimera software (Regents of University of California, USA) were used for the protein preparation. During this process, various adjustment has been made to the ligand and protein such as polar hydrogen atom were added, merging non-polar hydrogen atoms, setting solvation parameters followed by the inclusion of Gasteiger charges and the prepared structures were saved in (.pdbqt) format. For sdrE, the grid size was set to 80x89x79 Å, with grid centres at -5, 0.4, -1.7 Å. For CIfA, the grid size was 96x86x96 Å, with grid centres at 3, 0.4 and -7 Å. For FnBPA, the grid size was 89x87x100 Å, with grid centers at 23, 40 and 2 Å[13].

The docking experiment was performed with AutoDock Vina 1.5.7 in three independent molecular docking runs. After completing the molecular docking simulation, 10 ligand-protein models were generated and evaluated based on binding affinity. Finally, the ligand-receptor model that exhibit the most favourable binding energy and best interaction was selected for further visualization and analysis of their active interaction in 3D conformations by using BIOVIA Discovery Studio Visualiser 2021 (Dassault Systems, California, USA).

3. Results and Discussion

3.1. Chemistry

In this work, we synthesised the new dispiropyrrolidine oxindole derivatives in moderate to high yields (57–95%). All synthesised compounds were new except for the compounds **3**, **5a**, **5b**, **8a**, **8b**, **9a**, and **9b** which are known compounds that have been synthesised in our previous work[24]. The reaction was 1,3-dipolar cycloaddition reactions of azomethine ylides, which were generated *in situ* by the decarboxylative condensation of sarcosine **6** with isatin derivatives **7a-c**, in the presence of 3*E*,5*E*-bis(arylidene)-1-phenethyl-4-piperidone **5a-h** as dipolarophiles as shown in Scheme 1. The synthesised compounds **8-10** were characterised by spectroscopic methods, including ^{1}H and ^{13}C NMR, FT-IR, and HRMS analysis (see Supporting Information Figures S46-S165).

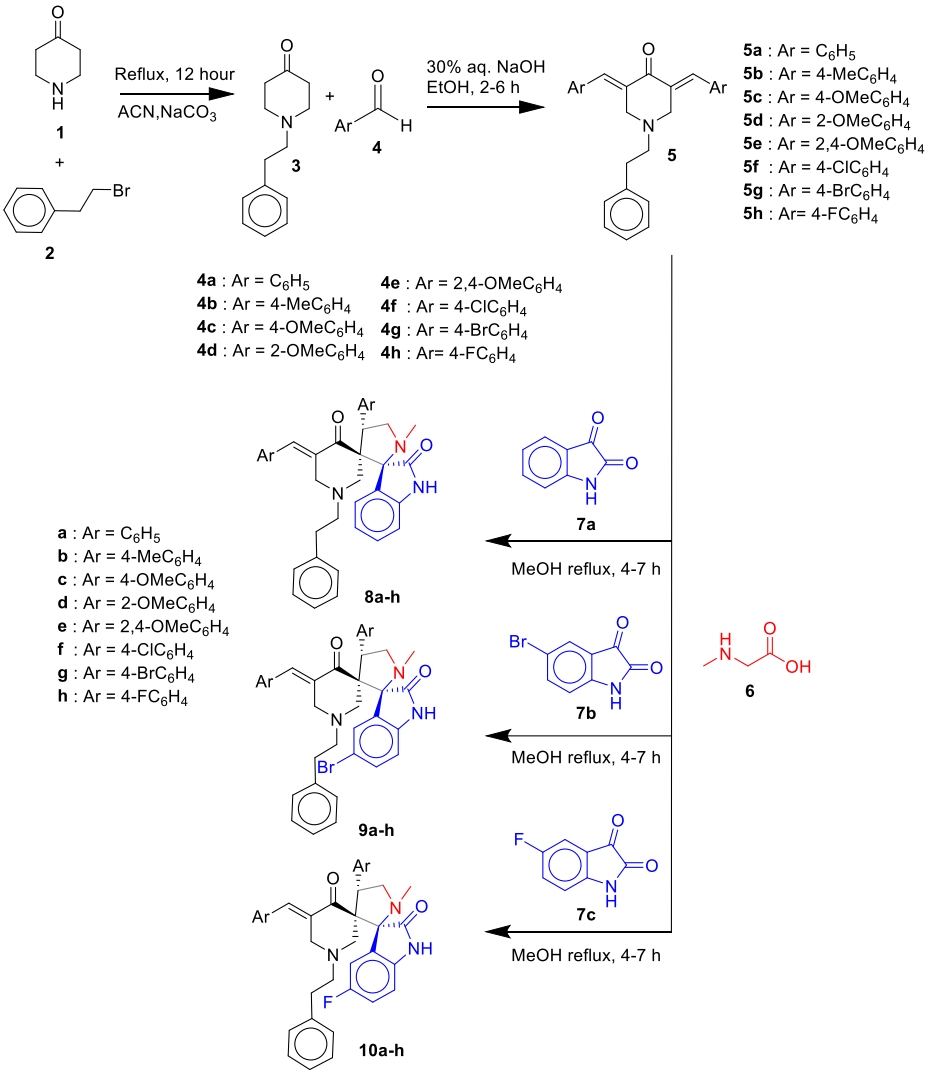

Scheme 1. Synthesis of dispiropyrrolidine oxindole derivatives **8-10**

Compound **9e** (Supporting information Figure S106-S110) has been selected as a representative example for discussion of spectral data. This compound exhibit peaks at 3193, 1709, 1593, and 1204 cm^{-1} corresponding to the peaks of N-H stretching, C=O stretching for ketone, C=C stretching of alkene and C-N stretching for tertiary amine group. In the ^{1}H NMR spectrum of compound **9e**, 41 total protons have been integrated within the range δ_H 1.79-10.59. Interestingly, on the piperidinyl proton CH_2-11, the chemical shift of the piperidinyl proton CH_2-11b is observed in the downfield region as a doublet at δ_H 2.97 (J=15.0 Hz). In contrast, the piperidinyl proton CH_2-11a appears in the upfield region as a doublet at δ_H 1.79 (J=15.0 Hz). This extreme upfield shift of the CH_2-11a proton is likely due to the anisotropic effect of the oxindole moiety on this neighbouring proton. In the case of proton CH_2-7a and CH_2-7b, proton CH_2-7b appeared as doublet at δ_H 3.28 (J=12.0 Hz) while proton CH_2-7a appeared to be doublet of doublet at δ_H 2.92 (J=12.0, 2.0 Hz). The coupling in proton CH_2-7a is due to geminal coupling between CH_2-7a and proton CH_2-7b (J=12.0 Hz) and long-range allylic coupling with olefinic methine C=CH-31, which appeared as doublet (J=2.0 Hz) at aromatic proton region (δ_H 7.65). On the other hand, pyrrolidinyl proton CH_2-13 appeared as two non-magnetically equivalent protons with doublet of doublet multiplicity. Chemical shift of proton CH_2-13a at δ_H 3.10 (J=8.0, 7.5 Hz) while for proton CH_2-13b is at δ_H 3.82 (J=8.0, 3.0 Hz). Both geminal proton CH_2-13 couple each other (J=8.0 Hz), and with vicinal methine proton CH-12 at δ_H 4.57 (J=7.5, 3.0 Hz). In the ^{13}C-NMR, a total of 41 carbon was

observed between δ_C 32.4-196.8. The signal for the spiro carbon C-10 and C-14 are observed at δ_C 62.9 and δ_C 76.0, respectively.

Furthermore, their relative configuration of chiral centres was established by comparing their key ^{13}C NMR chemical shift with that of closely related compounds, whose structures have been established by X-ray crystallography in earlier work[33,34].

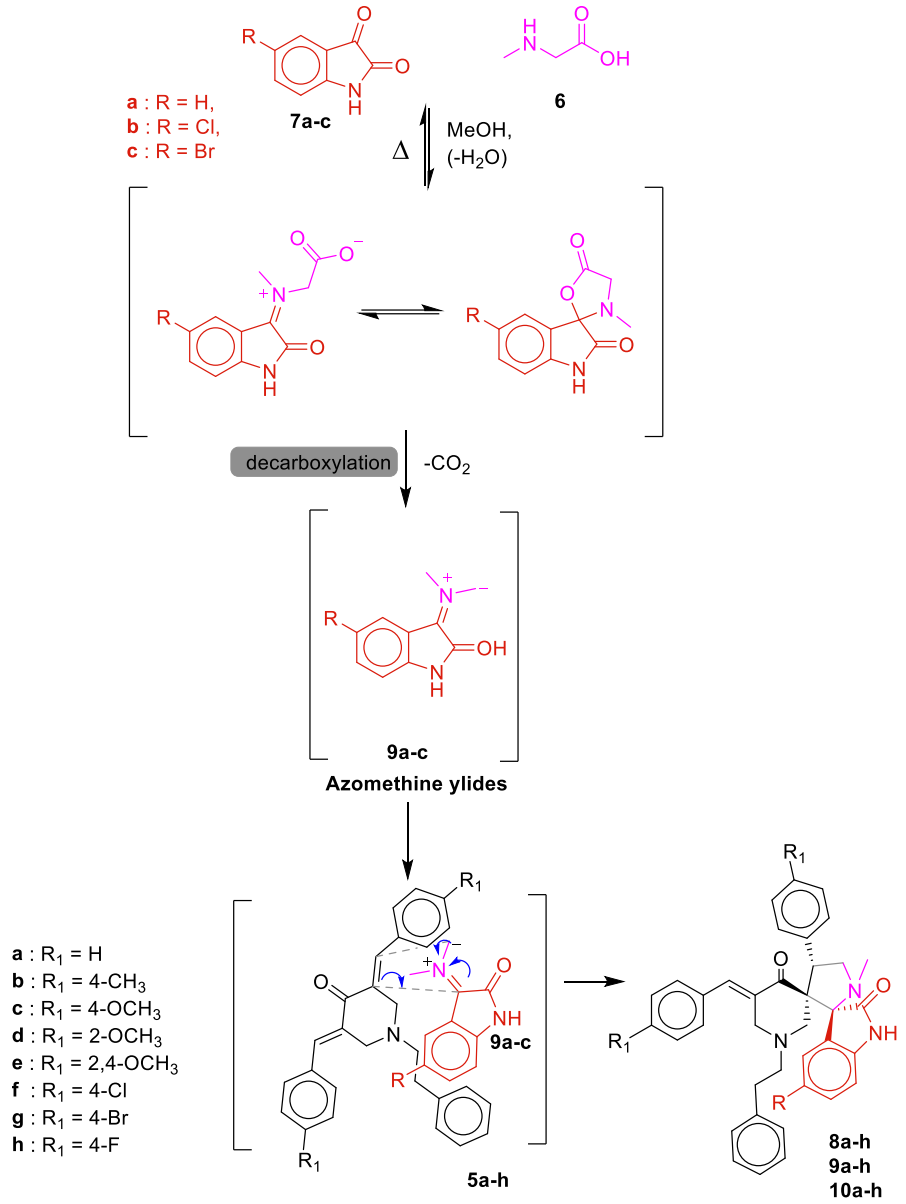

Scheme 2. Mechanism for the formation of dispiropyrrolidines derivatives **8-10**. (Adopted from our previous publication[24])

In our previous work, we has described the reaction mechanism of the dispiropyrrolidine oxindole compounds, as shown in[24]. First, sarcosine and the carbonyl group of isatin undergo a condensation reaction with the carbon at C-3, forming an iminium intermediate. This iminium intermediate is thought to be in equilibrium with a cyclic hemiaminal ester. It then irreversibly loses carbon dioxide to produce the key azomethine ylide species. Next, regio- and stereo-selective 1,3-dipolar cycloaddition of azomethine ylides with dipolarophiles will produce dispiropyrrolidine oxindole compounds, respectively. As the mechanism involves polar or charged species, methanol, a polar protic solvent, is chosen to ensure that the transition states of the intermediates are stabilised.

3.2. Biological Activity Assays

3.2.1 Anti bacteria inhibitory activity

The synthesised compounds **8-10** were screened for their *in-vitro* anti bacteria activity on Gram-positive and Gram-negative bacteria. Selected compounds with their minimum inhibitory concentration (MIC) and minimum bactericidal concentration (MBC) are shown in Table 1. Among the synthesised compounds, **9f** and **9g** exhibited moderate inhibitory activity against Gram-positive bacteria *Staphylococcus aureus* ATCC 25923 and *Staphylococcus aureus* ATCC 33591 (methicillin-resistant). The MIC and MBC values for **9f** and **9g** against these strains were determined to be 250 µg/mL and 325 µg/mL, respectively. In contrast, all synthesised compounds were ineffective against the Gram-negative bacteria tested, with MIC and MBC values exceeding 500 µg/mL. Compounds **9f** and **9g** shown to be selective inhibitors only for Gram-positive bacteria might be due to the difference in cell wall composition between Gram-positive and Gram-negative bacteria. The interaction and penetration of the synthesised compound might be facilitated by the thick peptidoglycan layer and its localization within the cell envelope of Gram-positive bacteria, leading to its effective microbial activity[32, 35]. Contrarily, the presence of lipopolysaccharide as the outer membrane and efflux pumps in Gram-negative bacteria likely to reduce the compound effectiveness[36].

Table 1. Minimum inhibitory concentration (MIC) and minimum bactericidal activity (MBC) of different microbes on dispiropyrrolidine oxindole derivatives **8-10**.

Compd.	***Staphylococcus aureus* ATCC 25923**		***Staphylococcus aureus* ATCC 33591**		***Escherichia coli* ATCC 35218**		***Pseudomonas aeruginosa* ATCC 27853**		***Salmonella typhimurium* ATCC 14028**	
	MIC (µg/mL)	MBC (µg/mL)	MIC (µg/mL)	MBC (µg/mL)	MIC (µg/mL)	MBC (µg/mL)	MIC (µg/mL)	MBC (µg/mL)	MIC (µg/mL)	MBC (µg/mL)
8a	>500	>500	>500	>500	>500	>500	>500	>500	>500	>500
8b	>500	>500	>500	>500	>500	>500	>500	>500	>500	>500
8c	>500	>500	>500	>500	>500	>500	>500	>500	>500	>500
8d	>500	>500	>500	>500	>500	>500	>500	>500	>500	>500
8e	>500	>500	>500	>500	>500	>500	>500	>500	>500	>500
8f	>500	>500	>500	>500	>500	>500	>500	>500	>500	>500
8g	>500	>500	>500	>500	>500	>500	>500	>500	>500	>500
8h	>500	>500	>500	>500	>500	>500	>500	>500	>500	>500
9a	>500	>500	>500	>500	>500	>500	>500	>500	>500	>500
9b	>500	>500	>500	>500	>500	>500	>500	>500	>500	>500
9c	>500	>500	>500	>500	>500	>500	>500	>500	>500	>500
9d	>500	>500	>500	>500	>500	>500	>500	>500	>500	>500
9e	>500	>500	>500	>500	>500	>500	>500	>500	>500	>500
9f	250	250	250	250	>500	>500	>500	>500	>500	>500
9g	350	350	350	350	>500	>500	>500	>500	>500	>500
9h	>500	>500	>500	>500	>500	>500	>500	>500	>500	>500
10a	>500	>500	>500	>500	>500	>500	>500	>500	>500	>500
10b	>500	>500	>500	>500	>500	>500	>500	>500	>500	>500
10c	>500	>500	>500	>500	>500	>500	>500	>500	>500	>500
10d	>500	>500	>500	>500	>500	>500	>500	>500	>500	>500
10e	>500	>500	>500	>500	>500	>500	>500	>500	>500	>500
10f	>500	>500	>500	>500	>500	>500	>500	>500	>500	>500
10g	>500	>500	>500	>500	>500	>500	>500	>500	>500	>500
10h	>500	>500	>500	>500	>500	>500	>500	>500	>500	>500

The MIC and MBC values obtained for MRSA strains remains the key potential of the compounds to be developed as therapeutics agent in the treatment of methicillin-resistance *Staphylococcus aureus*. Since MRSA can cause serious infection and resistance to several different class of antibiotics, it continues to be a major concern especially in healthcare environments around the world.

Even though the synthesised compounds show effectiveness against Gram-positive bacteria, its limited potential on Gram-negative strains such as *Escherichia coli*, *Pseudomonas aeruginosa*, *Salmonella typhimurium* can be considered for further exploration. Some modifications of the compounds structure such as introduction of new functional groups that able to target the outer membrane or efflux pumps mechanism, could lead to higher antimicrobial activity on both Gram-positive and Gram-negative bacteria[32].

3.3. Molecular Docking Studies

Based on biological assay study, compound **9f** and **9g** have shown a good to moderate potency in inhibiting *S. aureus*. Thus, both compounds have been selected to be further examine on their binding energy and their interaction between the compounds (ligand) and *S. aureus* adhesion proteins (receptor) through molecular docking studies. sdrE (PDB ID: 5WTA), CIfA (PDB ID:2VR3), and FnBPA (PDB ID: 4B5Z) are three important adhesion protein contributing to its ability to invade host cells, immune evasion and promoting biofilm formation to *S. aureus*[15, 16, 20].

Table 2. Binding energy of compound **9f** and **9g** with *S. aureus* adhesion protein

Protein (PDB ID)	Compound	Binding energy (kcal/mol)
FnBPA (4B5Z)	**9f**	-8.5 ± 0.00
	9g	-7.5 ± 0.20
CIfA (2VR3)	**9f**	-7.3 ± 0.10
	9g	-6.9 ± 0.07
sdrE (5WTA)	**9f**	-6.2 ± 0.03
	9g	-5.3 ± 0.00

Results are expressed as mean ± standard deviation (SD) for n=3 experiments

As shown in Figures 1a and Table 2, **9f** demonstrated the strongest binding energy for FnBPA, with a mean binding energy of -8.5±0.00 kcal/mol. This analogue interacts with several key residues such as ARG67, HIS61, ASP115, and PRO116, which contributes to its high binding stability. In contrast, **9g** showed lower mean binding energy of -7.5±0.2 kcal/mol than **9f**, indicating more variability in its interaction strength. **9g** interacts with key residue such as VAL306, LYS164 and VAL63. The role of FnBPA in adherence and cellular invasion has been studied in preclinical models of *S.aureus* infection and interaction with these specific residues may reduce *S. aureus* virulence and pathogenicity[37, 38]. In a study by Rafi Shaik et al. (2025)[39], mangostin-copper oxide complexes exhibited a binding energy of -7.9 kcal/mol against *S. aureus* FnBPA adhesion protein. The key amino acid residues involved in the interaction were GLN, PRO, TYR, HIS, ILE, VAL and PHE. Similar amino acid residues were observed in the binding interactions of **9f** and **9g.** Moreover, the binding energies of **9f** and **9g** are between -8.5 and -7.5 kcal/mol, which is close to the reported binding energy of -7.5 kcal/mol. This similarity highlights the potential of these compounds in inhibiting *S. aureus* strain bacteria.

For CIfA, Figure 1b and Table 2 shows the mean binding energy of **9f** is -7.3±0.1 kcal/mol with interaction key residue such as ASN57, ALA63, and ILE77. Compound **9g** exhibit lower binding energy -6.9±0.07 kcal/mol with interaction key residue such as ASN57 and ALA63. Even though **9g** shares common residue like ASN57, its binding interaction suggests less stability compared to **9f**. In sdrE protein, depicted in Figure 1c and Table 2, **9f** exhibit mean binding energy of -6.2±0.03 kcal/mol with interaction key residue such as ASN58, THR131 and ALA121. In contrast, **9g** exhibit lower binding energy of -5.3±0.00 kcal/mol with interaction key residue GLN434, TYR550, PRO437, PRO544 and ILE549. The conventional hydrogen bonding in **9f** might influence the higher binding energy than **9g** since a strong hydrogen bonding is crucial for most high-affinity ligand in ligand-protein complex[40]. Their key binding interaction between the ligand **9g** and **9f** with key amino acid are shown in Table 3.

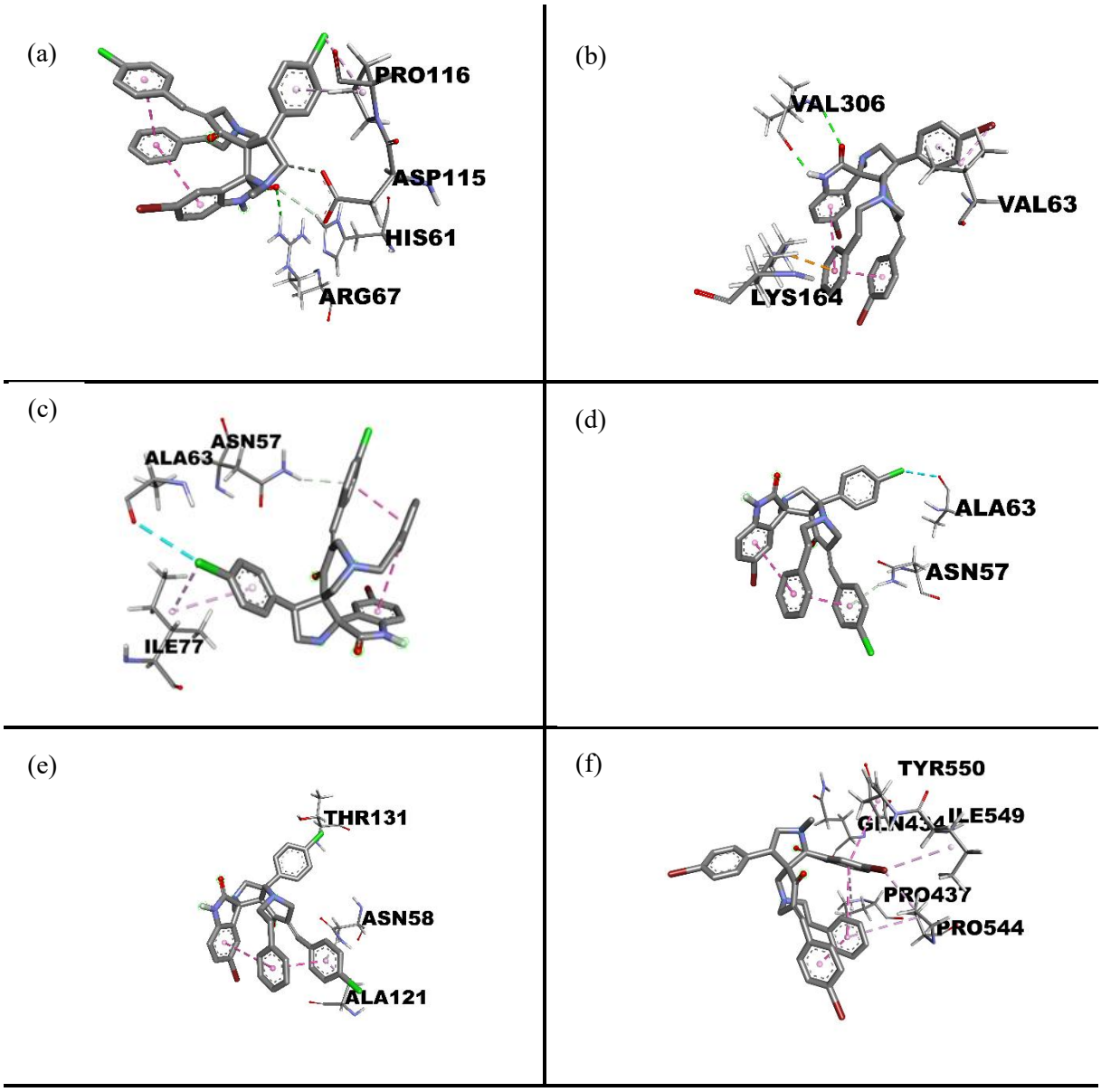

Figure 1. Binding interactions of compound **9f** (a) and **9g** (b) with FnBPA, **9f** (c) and **9f** (d) with CIfA and **9f** (e) and **9g** (f) with sdrE *S. aureus* adhesion proteins in 3D form.

Table 3. Key binding interactions of compounds **9f** and **9g** with FnBPA, CIfA and sdrE *S.aureus* adhesion protein

Protein	Compound	Protein residue	Interacting unit of compound	Types of interaction
FnBPA (PDB ID: 4B5Z)	**9f**	ARG67	C=O oxindoles	Conventional hydrogen bond (2.52Å)
		HIS61	C=O oxindoles	Carbon hydrogen bond
		ASP115	C-H pyrrolidines	Carbon hydrogen bond
		PRO116	Phenyl and Cl atom	π-π stacked
	9g	VAL306	C=O and N-H in oxindoles	Conventional hydrogen bond (2.57Å)
		LYS164	Phenyl	π-cation
		VAL63	Phenyl and bromo atom	Alkyl
CIfA (PDB ID: 2VR3)	**9f**	ALA63	Chloro atom	Halogen
		ASN57	Phenyl	π-donor hydrogen bond
		ILE77	Phenyl and chloro atom	Alkyl
	9g	ALA63	Bromo atom	Halogen
		ASN57	Phenyl	π-donor hydrogen bond
sdrE (PDB ID: 5WTA)	**9f**	THR131	Chloro atom	Carbon hydrogen bond
		ASN58	Phenyl	π-donor hydrogen bond
		ALA121	Phenyl	π-alkyl
	9g	GLN434	N-H oxindoles	Conventional hydrogen bond (1.87Å)
		TYR550	Phenyl	π-π T-shaped
		PRO544	Bromo atom	Alkyl
		ILE549	Bromo atom	Alkyl
		PRO437	Phenyl	π alkyl
		PRO544	Phenyl	π alkyl

3.4. Structure-Activity Relationship (SAR)

The SAR was established by synthesising dispiropyrrolidine oxindole derivatives containing electron donating and withdrawing groups on the phenyl ring, as well as different halogen groups (Cl and Br) on oxindoles moiety. Among all the derivatives, only **9f** and **9g** exhibited moderate MRSA activity. The 4-chlorophenyl derivative **9f** (MIC and MBC: 250 µg/mL) was more potent than the 4-bromophenyl derivative **9g** (MIC and MBC: 350 µg/mL). Compound **9f** showed better inhibitory activity which might be due to the presence of two chlorine atoms on the phenyl ring. Interestingly, when both chlorine atom was replaced with bromine atom and fluorine atom in the same para position, MRSA inhibition significantly decrease (MIC and MBC: >350 µg/mL for bromine, >500 µg/mL for fluorine). This indicates that the presence of two chlorine atoms on the phenyl ring is crucial for inhibiting MRSA and replacing with more and less electronegative halogen atom will reduce its inhibitory activity. The molecular docking study also suggests that the two chlorine atoms interact with key residues of all three proteins amino acid residue (FnBPA, CIfA, sdrE) such as PRO116 (π-π stacked), ALA63 (halogen) and THR131 (hydrogen bonding). On the other hand, the bromine atom in the oxindole moiety is essential for inhibition, as replacing the bromine atom with a fluorine or hydrogen atom, significantly decreases MRSA inhibition to more than 500 µg/mL for both MIC and MBC. Figure 2 summarizes the structure-activity relationship studies of these dispiropyrrolidine oxindole compounds.

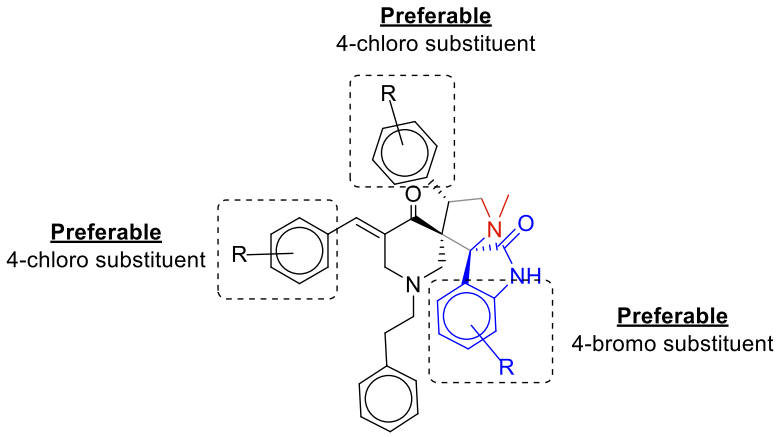

Figure 2. SAR study of dispiropyrrolidine oxindole compounds

4. Conclusion

In summary, we have successfully synthesised dispiropyrrolidine oxindole derivatives with promising potency to inhibit MRSA. The SAR study suggests that the chlorine atoms at *para* position on the phenyl ring and bromine atom in position 5 in oxindoles moiety were the most preferable halogens that may contribute in inhibiting MRSA activity. Additionally, a molecular docking study conducted on MRSA adhesion proteins provides further insight into the interaction between the dispiropyrrolidine oxindole compounds and their target *S. aureus* adhesion proteins. These findings confirm the interaction of our synthesised compounds with MRSA adhesion proteins as well as the suitability of the chlorine atom in *para* position on the phenyl ring and the bromine atom at position 5 in the oxindoles moiety. Further work on evaluation of the FnBPA gene expression and protein will confirm the involvement of this adhesion protein in its inhibitory effect. This allowed computational, medical and synthetic chemists to further develop high performance anti-MRSA drugs based on dispiropyrrolidine oxindole derivatives.

Acknowledgements

The authors would like to acknowledge the financial support from Ministry of Higher Education (MOHE) under the Fundamental Research Grant Scheme (FRGS) FRGS/1/2023/STG04/USM/02/3 The authors sincerely thank Universiti Sains Malaysia (USM) and the NPSO Laboratory for the facilities used in this research work.

Supporting Information

Supporting information accompanies this paper on http://www.acgpubs.org/journal/organic-communications

ORCID
Mohd Khairul Nizam Mazlan: 0000-0003-3903-2563
Mohamad Nurul Azmi: 0000-0002-2447-0897
Saiful Azmi Johari: 0000-0003-3898-2524
Nor Syaidatul Akmal Mohd Yousof: 0000-0003-1375-2984
Mohammad Tasyriq Che Omar: 0000-0002-1294-7520
Habibah A. Wahab: 0000-0002-8353-8679
Mohd Fazli Mohammat: 0000-0002-6926-0447

References

[1] Lin, J.-Y.; Lai, J.-K.; Chen, J.-Y.; Cai, J.-Y.; Yang, Z.-D.; Yang, L.-Q.; Zheng, Z.-T.; Guo, X.-G. Global insights into MRSA bacteremia: A bibliometric analysis and future outlook. *Front. Microbiol.* **2025**, *15*, 1516584.

[2] World Health Organization. WHO bacterial priority pathogens list 2024: Bacterial pathogens of public health importance to guide research, development and strategies to prevent and control antimicrobial resistance. **2024**, 1-72.

[3] Ministry of Health Malaysia. National surveillance on antimicrobial resistance (NSAR) report. **2024**, 1-58.

[4] Band, V. I.; Weiss, D. S. Heteroresistance to beta-lactam antibiotics may often be a stage in the progression to antibiotic resistance. *PLoS Biol.* **2021**, *19* (*7*), 3001346.

[5] Miklasinska-Majdanik, M. Mechanisms of resistance to macrolide antibiotics among *Staphylococcus aureus*. *Antibiotics* **2021**, *10* (*11*), 1406.

[6] Lund, D.; Coertze, R. D.; Parras-Molto, M.; Berglund, F.; Flach, C.-F.; Johnning, A.; Larsson, D. G. J.; Kristiansson, E. Extensive screening reveals previously undiscovered aminoglycoside resistance genes in human pathogens. *Commun. Biol.* **2023**, *6* (*1*), 812.

[7] Hamady, A. B.; Abd El-Fadeal, N. M.; Imbaby, S.; Nassar, H. M. A.; Sakr, M. G.; Marei, Y. E. Expression of norA, norB and norC efflux pump genes mediating fluoroquinolones resistance in MRSA isolates. *J. Infect. Dev. Ctries.* **2024**, *18* (*3*), 399-406.

[8] Acharya, Y.; Bhattacharyya, S.; Dhanda, G.; Haldar, J. Emerging roles of glycopeptide antibiotics: moving beyond gram-positive bacteria. *ACS Infect. Dis.* **2022**, *8* (*1*), 1-28.

[9] Mahjabeen, F.; Saha, U.; Mostafa, M. N.; Siddique, F.; Ahsan, E.; Fathma, S.; Tasnim, A.; Rahman, T.; Faruq, R.; Sakibuzzaman, M.; Dilnaz, F.; Ashraf, A. An update on treatment options for methicillin-resistant *Staphylococcus aureus* (MRSA) bacteremia: A systematic review. *Cureus* **2022**, *14* (*11*), 31486.

[10] Tsutsuura, M.; Moriyama, H.; Kojima, N.; Mizukami, Y.; Tashiro, S.; Osa, S.; Enoki, Y.; Taguchi, K.; Oda, K.; Fujii, S.; Takahashi, Y.; Hamada, Y.; Kimura, T.; Takesue, Y.; Matsumoto, K. The monitoring of vancomycin: A systematic review and meta-analyses of area under the concentration-time curve-guided dosing and trough-guided dosing. *BMC Infect. Dis.* **2021**, *21* (*1*), 153.

[11] Lewis, P. O.; Heil, E. L.; Covert, K. L.; Cluck, D. B. Treatment strategies for persistent methicillin-resistant *Staphylococcus aureus* bacteraemia. *J. Clin. Pharm. Ther.* **2018**, *43* (*5*), 614-625.

[12] Cosimi, R. A.; Beik, N.; Kubiak, D. W.; Johnson, J. A. Ceftaroline for severe methicillin-resistant *Staphylococcus aureus* infections: A systematic review. *Open Forum Infect. Dis.* **2017**, *4* (*2*), 84.

[13] Che Omar, M. T.; Musthafa Kamal, M. F.; Azmi, M. N. Exploration of benzhydrol analogues of 1′-acetoxychavicol acetate as potential inhibitors of sdrE adhesion protein in *Staphylococcus aureus*: Antimicrobial activity and multi-computational analysis. *Comp. Biol. Chem.* **2026**, *120*, 108618.

[14] Zuo, Q.-F.; Cai, C.-Z.; Ding, H.-L.; Wu, Y.; Yang, L.-Y.; Feng, Q.; Yang, H.-J.; Wei, Z.-B.; Zeng, H.; Zou, Q.-M. Identification of the immunodominant regions of *Staphylococcus aureus* fibronectin-Binding protein A. *PloS one* **2014**, *9* (*4*), 95338.

[15] Zhang, Y.; Wu, M.; Hang, T.; Wang, C.; Yang, Y.; Pan, W.; Zang, J.; Zhang, M.; Zhang, X. *Staphylococcus aureus* sdrE captures complement factor H's C-terminus via a novel ‘close, dock, lock and latch' mechanism for complement evasion. *Biochem. J.* **2017**, *474* (*10*), 1619-1631.

[16] Ganesh, V. K.; Rivera, J. J.; Smeds, E.; Ko, Y. P.; Bowden, M. G.; Wann, E. R.; Gurusiddappa, S.; Fitzgerald, J. R.; Höök, M. A structural model of the Staphylococcus aureus ClfA-fibrinogen interaction opens new avenues for the design of anti-staphylococcal therapeutics. *PLoS Pathog* **2008**, *4* (*11*), e1000226.

[17] Banerjee, B.; Emolo, C.; Shi, M.; Al Fardan Abrar, A.; Pius, T.; Azam Muhammad, S.; McAdow, M.; Schneewind, O.; Missiakas, D. Inhibitory activities of monoclonal antibodies against *Staphylococcus aureus* clumping factor A. *mBio* **2025**, *16* (*10*), e02197-02125.

[18] Da Costa, T. M.; Viljoen, A.; Towell, A. M.; Dufrêne, Y. F.; Geoghegan, J. A. Fibronectin binding protein B binds to loricrin and promotes corneocyte adhesion by Staphylococcus aureus. *Nat. Commun.* **2022**, *13* (*1*), 2517.

[19] Gondokaryono, S. P.; Ushio, H.; Niyonsaba, F.; Hara, M.; Takenaka, H.; Jayawardana, S. T. M.; Ikeda, S.; Okumura, K.; Ogawa, H. The extra domain A of fibronectin stimulates murine mast cells via Toll-like receptor 4. *J. Leukocyte Bioli* **2007**, *82* (*3*), 657-665.

[20] Kong, L. X.; Wang, Z.; Shou, Y. K.; Zhou, X. D.; Zong, Y. W.; Tong, T.; Liao, M.; Han, Q.; Li, Y.; Cheng, L.; Ren, B. The FnBPA from methicillin-resistant *Staphylococcus aureus* promoted development of oral squamous cell carcinoma. *J. Oral. Microbiol.* **2022**, *14* (*1*), 2098644.

[21] Chupakhin, E.; Babich, O.; Prosekov, A.; Asyakina, L.; Krasavin, M. Spirocyclic motifs in natural products. *Molecules* **2019**, *24* (*22*), 4165.

[22] Aldeghi, M.; Malhotra, S.; Selwood, D. L.; Chan, A. W. E. Two and three-dimensional rings in drugs. *Chem. Biol. Drug Des.* **2014**, *83* (*4*), 450-461.

[23] Azmi, M.N.; Tan, C.S.; Abdulameed, H.T., Kamal, N.N.S.N.M.; Kahar, N.E.A.; Omar, M.T.C. Synthesis of benzhydrol analogues based on 1′-acetoxychavicol acetate (ACA), as a stable and potent antiproliferative agent on breast cancer cell lines, ADMET analysis and molecular docking study. *Org. Commun.* **2024**, *17* (*4*), 99-114.

[24] Mohamed Yusoff, N.; Osman, H.; Katemba, V.; Abd Ghani, M. S.; Supratman, U.; Che Omar, M. T.; Murugaiyah, V.; Xiang, R.; Six, Y.; Azmi, M. N. Design, synthesis and cholinesterase inhibitory activity of new dispiro pyrrolidine derivatives. *Tetrahedron* **2022**, *128*, 133115.

[25] Alkaltham, M. F.; Almansour, A. I.; Arumugam, N.; Vagolu, S. K.; Tønjum, T.; Alaqeel, S. I.; Rajaratnam, S.; Sivaramakrishnan, V. Activity against *Mycobacterium tuberculosis* of a new class of spirooxindolopyrrolidine embedded chromanone hybrid heterocycles. *RSC Adv.*. **2024**, *14* (*17*), 11604-11613.

[26] Areej, M. J.; Jalal, A. Z.; Mustafa, M. E.-A.; Mohammed, M. A.-M.; Salim, S. S.; Violet, K.; Randa, N. H. Evaluation of spirooxindole-3,3'-pyrrolines-incorporating isoquinoline motif as antitumor, anti-inflammatory, antibacterial, antifungal, and antioxidant agents. *Anti-Inflamm. Anti-Allergy Agents Med. Chem.*. **2024**, *23* (*4*), 261-272.

[27] Lopes, E. A.; Mestre, R.; Fontinha, D.; Legac, J.; Pei, J. V.; Sanches-Vaz, M.; Mori, M.; Lehane, A. M.; Rosenthal, P. J.; Prudêncio, M.; Santos, M. M. M. Discovery of spirooxadiazoline oxindoles with dual-stage antimalarial activity. *Eur. J. Med. Chem* **2022**, *236*, 114324.

[28] Leena, S. S.; Akhir, A.; Saxena, D.; Maitra, R.; Chopra, S.; Deepthi, A. Synthesis of tryptanthrin appended dispiropyrrolidine oxindoles and their antibacterial evaluation. *RSC Med. Chem.* **2023**, *14* (*6*), 1165-1171.

[29] Zhou, L.-M.; Qu, R.-Y.; Yang, G.-F. An overview of spirooxindole as a promising scaffold for novel drug discovery. *Expert Opin. Drug Discov.* **2020**, *15* (*5*), 603-625.

[30] Zhuang, T.; Xiong, J.; Ren, X.; Liang, L.; Qi, Z.; Zhang, S.; Du, W.; Chen, Y.; Liu, X.; Zhang, G. Benzylaminofentanyl derivates: Discovery of bifunctional opioid and receptor ligands as novel analgesics with reduced adverse effects. *Eur. J. Med. Chem* **2022**, *241*, 114649.

[31] Ashraf Ali, M.; Sanjeevi Lakshmipathi, V.; Beevi, F.; Suresh Kumar, R.; Ismail, R.; Soo Choon, T.; Chee Wei, A.; Keng Yoon, Y.; Basiri, A. Antimycobacterial activity: Synthesis and biological evaluation of novel substituted (3*E*,5*E*)-3,5-diarylidene-1-phenethylpiperidine-4-one derivatives. *Lett. Drug Des. Discov.* **2013**, *10* (*5*), 471-476.

[32] Md. Salleh, S. N.; Abdullah, M. Z.; Mohamed Saheed, M. S.; Mohammat, M. F. Antimicrobial and antiviral effect of cellulose acetate nanofibres doped with pyrrolidone against methicillin-resistant *Staphylococcus aureus* (MRSA) and human coronavirus 229E (HCoV-229E). *J. Hazard. Mater. Adv.* **2025**, *17*, 100598.

[33] Li, X.; Yu, X.; Yi, P. Synthesis of novel trispiroheterocycles through 1,3-dipolar cycloaddition of azomethine ylides and nitrile oxide. *Chin. J. Chem.* **2010**, *28* (*3*), 434-438.

[34] Girgis, A. S.; Panda, S. S.; Farag, I. S. A.; El-Shabiny, A. M.; Moustafa, A. M.; Ismail, N. S. M.; Pillai, G. G.; Panda, C. S.; Hall, C. D.; Katritzky, A. R. Synthesis, and QSAR analysis of anti-oncological active spiro-alkaloids. *Org. Biomol. Chem.* **2015**, *13* (*6*), 1741-1753.

[35] Çelik, F.; Ünver, Y.; Aydin, A.; Güler, H.İ.; Bektaş, K.I. Synthesis, characterization and biological activity of novel ionic liquids with bis-imidazole moieties: antitumor, antimicrobial effects and molecular docking studies. *Org. Commun.* **2024**, *17* (*1*), 23-37.
[36] Gaurav, A.; Bakht, P.; Saini, M.; Pandey, S.; Pathania, R. Role of bacterial efflux pumps in antibiotic resistance, virulence, and strategies to discover novel efflux pump inhibitors. *Int. J. Syst. Evol. Microbiol.* **2023**, *169* (*5*), 001333.
[37] Edwards, A. M.; Potts, J. R.; Josefsson, E.; Massey, R. C. *Staphylococcus aureus* host cell invasion and virulence in sepsis is facilitated by the multiple repeats within FnBPA. *PLoS Pathog.* **2010**, *6* (*6*), 1000964.
[38] Shinji, H.; Yosizawa, Y.; Tajima, A.; Iwase, T.; Sugimoto, S.; Seki, K.; Mizunoe, Y. Role of fibronectin-binding proteins A and B in *in vitro* cellular infections and *in vivo* septic infections by *Staphylococcus aureus*. *Infect. Immun.* **2011**, *79* (*6*), 2215-2223.
[39] Rafi Shaik, M.; Ramasamy, M.; Jain, D.; Muthu, K.; Manivannan, C.; Althaf Hussain, S.; Deepak, P.; Thiyagarajulu, N.; Guru, A.; Perianaika Matharasi Antonyraj, A.; Melo Coutinho, H. D. Dual action of nanostructured α-mangostin-copper oxide complexes against dental pathogen biofilms and oral cancer via apoptosis gene modulation. *Chem. Biodivers.* **2025**, *22* (*3*), 202401961.
[40] Raschka, S.; Wolf, A. J.; Bemister-Buffington, J.; Kuhn, L. A. Protein–ligand interfaces are polarized: Discovery of a strong trend for intermolecular hydrogen bonds to favor donors on the protein side with implications for predicting and designing ligand complexes. *J. Comput. Aided Mol. Des.* **2018**, *32* (*4*), 511-528.